

Transesterification of Waste Cooking Oil Utilizing Heterogeneous K_2CO_3/Al_2O_3 and KOH/Al_2O_3 Catalysts

Muhammad Amirrul Hakim Lokman Nohakim¹, Norshahidatul Akmar Mohd Shohaimi^{1*}, Mohd Lokman Ibrahim^{2,3}, Wan Nur Aini Wan Mokhtar⁴ and Ahmad Zamani Ab Halim⁵

¹Faculty of Applied Science, Universiti Teknologi MARA Cawangan Pahang, Kampus Jengka, 26400 Bandar Tun Abdul Razak, Pahang, Malaysia

²Centre for Functional Materials and Nanotechnology, Institute of Science, Universiti Teknologi MARA, 40450 Shah Alam, Selangor, Malaysia

³School of Chemistry and Environment, Faculty of Applied Sciences, Universiti Teknologi MARA, 40450 Shah Alam, Selangor, Malaysia

⁴Department of Chemical Sciences, Faculty of Science and Technology, Universiti Kebangsaan Malaysia, 43600 UKM Bangi, Selangor, Malaysia

⁵Faculty of Industrial Sciences & Technology, Universiti Malaysia Pahang, Kuantan, Pahang, Malaysia

*Corresponding author (e-mail: akmarshohaimi@uitm.edu.my)

Biodiesel production from waste oil is preferable these days as the amount of fossil fuel available for diesel production is decreasing year by year. In this study, the transesterification of waste cooking oil was performed, producing simple alkyl esters from the chemical reaction of triglycerides and methanol, supported by a heterogeneous catalyst to speed up the reaction. Potassium carbonate (K_2CO_3) and potassium hydroxide (KOH) catalysts loaded at concentrations of 10% and 30% on an aluminium oxide (Al_2O_3) support were prepared by the incipient wetness impregnation (IWI) method. The feedstock used was waste cooking oil (WCO) collected from households, with a free fatty acid (FFA) value of 1.05 and a moisture content of less than 0.015%. The catalysts were extensively investigated using Thermogravimetric analysis (TGA), X-Ray Diffraction Spectroscopy (XRD) and Brunauer-Emmett-Teller (BET) analysis, while the ester content of the biodiesel produced was characterised using Gas Chromatography-Mass Spectroscopy (GC-MS). The operating conditions for the transesterification reaction included an oil to methanol ratio of 1:12, catalyst loading of 5 wt%, and reaction temperature of 65°C. It was found that 10 wt% K_2CO_3/Al_2O_3 was the best catalyst, yielding 9.86g (98.6%) of biodiesel, with a conversion of 81.92% of ester content that made the total biodiesel yield equal to 8.75g (87.57%). These catalysts showed promising results in converting the triglycerides in waste oil to fatty acid methyl esters (FAME).

Key words: Biodiesel; transesterification; aluminium oxide; waste cooking oil

Received: November 2020; Accepted: January 2021

The rising demand for petroleum is a consequence of the increase in world population and hence economic development. Biofuel production has recently come into the limelight as an alternative source of fuel because of the depletion of fossil fuel reserves and its related environmental issues [1]. Biodiesel or Fatty Acid Methyl Esters (FAME) is a promising bioenergy source that can reduce emissions and is accepted globally as an alternative to petroleum. Biodiesel is a realistic solution because it is non-toxic, releases no harmful emissions and is a renewable resource [2]. Biodiesel is commonly produced by the esterification or transesterification of vegetable oils or animal fats with methanol using a suitable catalyst [3,4]. While biodiesel offers several advantages over conventional diesel fuel, it has not been commercially successful in many countries, including Indonesia and Malaysia, due to a lack of adequate feedstock. Using vegetable oil and animal fat for biodiesel production is a matter

of concern because it can affect food production [5]. Thus, food-based feedstock should preferably be substituted with low quality non-edible feedstock for biodiesel production.

Waste cooking oil (WCO) obtained from domestic waste can serve as a possible replacement for vegetable oils and animal fats because it can minimize the total cost of biodiesel production and effectively solve the problems of WCO disposal [6]. The catalyst used in esterification is usually a homogeneous acid catalyst [7] while transesterification uses a homogeneous base catalyst [8]. In recent years, the production of biodiesel from heterogeneous catalysts has been widely studied as it is environmentally friendly, has good reusability and it is easy to separate the catalyst from the product [9]. After careful studies on a variety of heterogeneous catalytic derivatives reported in the literature [9–18], potassium is a

potential metal to be investigated [10,12–17,19–21]. Potassium hydroxide (KOH) and potassium carbonate (K_2CO_3) immobilized onto powdered alumina (Al_2O_3) are good catalysts for the transesterification of different feedstocks to FAME due to their easy preparation and low cost [22,23]. Both catalysts were also found to be the strongest base catalysts. The concentration of the catalyst is important as the feedstock used generally has high FFA values. Evangelista *et al.*, [18] reported that K_2CO_3/Al_2O_3 and KOH/Al_2O_3 was suitable for high quality feedstock such as sunflower oil [24], canola oil [25] and rapeseed oil [26]. The catalyst also needs to be tested by using low quality feedstock such as WCO.

A major issue with homogeneous catalysts is that, under certain reaction conditions, they may cause emulsion problems which can affect the transesterification process [27]. Thus, the aim of this study is to investigate KOH/Al_2O_3 and K_2CO_3/Al_2O_3 powder catalysts to verify their potential in the transesterification process of WCO. In this study, the powdered KOH/Al_2O_3 and K_2CO_3/Al_2O_3 catalysts were prepared in 10 wt% and 30 wt% concentrations. The application of Al_2O_3 as a support for powdered heterogeneous catalysts offers benefits because of its unique physical and chemical properties [28]. Moreover, the high catalytic activity of the catalyst is due to the increased surface area and greater concentration of highly reactive sites [5]. Moreover, these catalysts can be recycled several times, for example $K_2O/\gamma-Al_2O_3$ [29], $KI/\gamma-Al_2O_3$ [13] and KOH/Al_2O_3 [30] which have been synthesized by previous researchers using different types of feedstock.

The prepared powder catalyst was characterized using Thermogravimetric analysis (TGA), X-Ray Diffraction Spectroscopy (XRD) and Brunauer-Emmett-Teller (BET) analysis. The catalyst concentration was varied, while other conditions for the transesterification process were set as constant (oil:methanol ratio of 1:12, catalyst loading of 5 wt%, reaction temperature of 65°C and reaction time of 3 hours). After the biodiesel conversion was obtained, the yield (ester content) was determined by using Gas Chromatography-Mass Spectroscopy (GC-MS).

METHODOLOGY

Materials

WCO feedstock was obtained from households in Kawasan Perindustrian Pasir Gudang, Johor. The WCO was pre-treated first by heating at 100°C for 1 hour, and then filtered to remove traces of water and suspended particles. The aluminium oxide powder support (Al_2O_3 , < 1 nm) was obtained from Sigma-Aldrich (commercial grade). Potassium carbonate (K_2CO_3 , 99%) was obtained from Merck. Methanol (CH_3OH , 99%) was analytical grade (AR) and methyl heptadecanoate ($C_{18}H_{36}O_2$, 99%) for GC-MS internal standards were obtained from Sigma-Aldrich. The perforated hydrophilic materials (PHM) were made from Low Density Polyethylene (LDPE) plastic that has been proven tough and thermally stable for the reaction. For free fatty acid (FFA) and saponification (SV) testing: sodium hydroxide (NaOH, 99%), phenolphthalein ($C_{20}H_{14}O_4$, 99%) and hydrochloric acid (HCl, 32%) were obtained from QReC.

Feedstock Characterization

Waste cooking oil was characterized in terms of acid value, saponification value, free fatty acid value, viscosity and moisture content. Table 1 shows the test methods used to determine the properties of the oil.

Saponification value (SV) was determined to obtain the molecular weight of the WCO. Molecular weight is important to determine the suitable oil to methanol ratio. Free fatty acid (FFA) analysis was performed to determine the most suitable method for biodiesel production. If the FFA value for the feedstock is higher than 5, the best method would be esterification and if it is less than 5, transesterification is more suitable. The feedstock moisture (from Karl fisher) needs to be less than 0.05 to avoid water molecules inhibiting FAME conversion [21].

Catalyst Preparation

The K_2CO_3/Al_2O_3 and KOH/Al_2O_3 powder catalysts with 10% and 30 wt% concentrations were prepared by the incipient wetness impregnation (IWI) method on an Al_2O_3 powder support in an aqueous solution of salt.

Table 1. Standard test methods used to determine properties of oil for biodiesel production

Test	Method
Acid Value	ASTM D664/D8045-17e1
Saponification Value	ASTM D94
Free Fatty Acid Value	ASTM D5555-95
Viscosity	ASTM D445/D446
Moisture	ASTM D5556-19

In this study, the salt solution was added dropwise into a beaker containing alumina powder immersed in distilled water. The mixture was then stirred continuously while heating until the solution became concentrated. The prepared catalyst was dried in an oven at $90^\circ C$ overnight and then calcined at $700^\circ C$ with a ramp rate of $15^\circ C/min$ for 3 hours. Equation 1 was used to determine the catalyst concentration where x refers to the desired concentration, y refers to the WCO weight in grams (g), and z refers to the molecular weight of salt used.

$$\text{Catalyst concentration, wt\%} = \frac{x}{100} \times y \times \frac{z}{\text{mw of K}} \quad (1)$$

Catalyst Characterization

Thermogravimetric analysis (TGA) with DTG curves was used for the analysis of the thermal decomposition of the catalyst. The calcination temperature for the catalyst was determined based on the maximum thermal decomposition shown by TGA-DTG curves. Thermogravimetric analysis was performed using a thermal gas detector GSA7 from Perkin Elmer. Around 5 mg of sample was heated from ambient temperature to $1000^\circ C$ with a heating rate of $15^\circ C/min$ in an inert nitrogen atmosphere with a gas flow rate of 20 ml/min.

X-ray diffraction (XRD) analysis was used for identification and characterization of the internal structure, bulk phase, and the composition of crystalline phases of the catalyst [31]. The analysis was carried out using X'Pert PRO Theta from PANalytical with a diffracted beam monochromator, using a step scan mode with range $0^\circ-90^\circ$ of 2θ with phase size 0.0334° and a time per step of 100 seconds using $Cu K\alpha$ radiation ($\lambda=0.154056$ nm) with 40kV

working voltage and 100 mA current. Nitrogen adsorption/desorption analysis was performed using Micrometrics ASAP 2010 from USA to determine the catalyst surface area and pore type. Prior to the analysis, the sample was degassed and heated for 24 h at $120^\circ C$. For pore size and volume, Barrett-Joyner-Halenda (BJH) analysis was performed based on the kelvin equation.

Transesterification Process

10 grams of WCO was weighed and placed in a 50 mL two-necked round bottom flask. The WCO was heated to $65^\circ C$ and the desired amount of methanol (at a 1:12 ratio) was added. The 30 wt% of catalyst was weighed and added into the PHM before the transesterification process. Figure 1 shows a schematic representation of the transesterification process.

The reaction flask acts like a pseudo-fixed BET character and the material was chemically inert and thermally stable. The solution was mixed using a magnetic stirrer at 300 rpm for 3 hours. After the reaction was complete, it was cooled to room temperature and the powder catalyst was immediately separated from the mixture using a separating funnel. Two layers were observed: the bottom layer was glycerol and the top layer was biodiesel. The mixture containing the powder catalyst was then transferred into a 15 mL centrifuge tube and centrifuged at 4500 rpm for 5 minutes. The catalyst (bottom layer) and glycerol phase (middle layer) were removed and placed in a separate container. The biodiesel (top layer) was washed with hot water to remove excess glycerol and methanol. It was then heated at $100^\circ C$ for several minutes until the bubbles disappeared, to remove excess water. Finally, the biodiesel was weighed and sent for gas chromatography analysis.

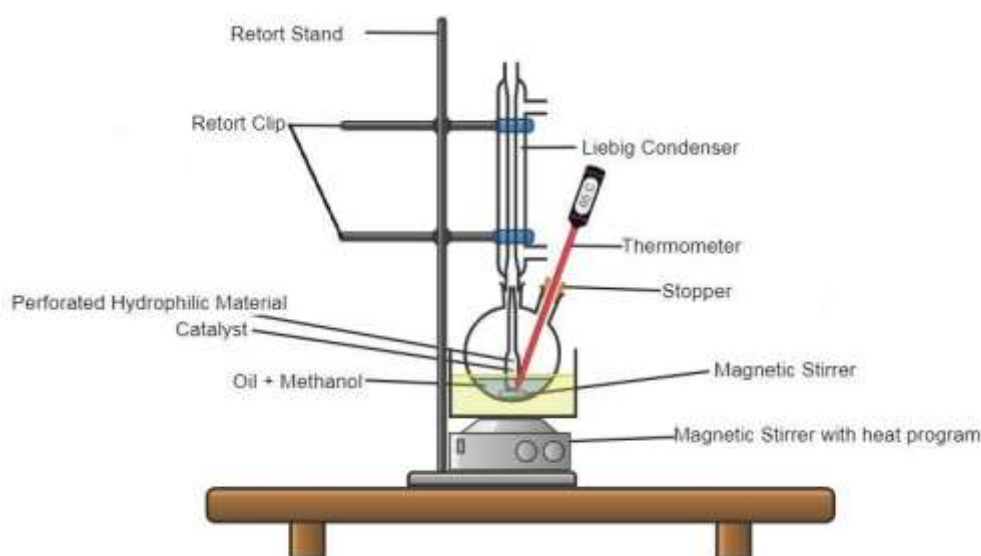


Figure 1. Schematic representation of the transesterification process with application of perforated hydrophilic material (PHM) in the reaction flask

Determination of Ester Content using Gas Chromatography-Mass Spectroscopy (GCMS)

The biodiesel collected from the transesterification process was evaluated by GC-MS (Agilent model). The injector and detector temperature were set at 240°C. The gas carrier was helium with a flow rate of 19.2 mL/min. The column temperature was set to 150°C with ramp rate 15°C/min for warm up. On starting the instrument, the column temperature was set at 300°C with ramp rate 7 °C/min. 1 µL of sample was injected in the GC inlet port. The peak area of FAME present in the biodiesel was determined from the chromatograph and compared with the peak area of the internal standard (methyl heptadecanoate).

The percentage of impure biodiesel from the transesterification process was determined using Equation 2.

$$\% \text{ biodiesel conversion, } A = \frac{\text{Mass of biodiesel collected (g)}}{10 \text{ g of WCO}} \times 100\% \quad (2)$$

The percentage of ester content in the biodiesel sample was determined after obtaining the percentage of impure biodiesel. This is because the impure biodiesel contains some unreacted oil, glycerol and other impurities [32]. The formula to calculate the ester content is provided by the Agilent standard method EN14103 [33] as follows:

$$c = \frac{TA-AEI}{AEI} \times \frac{CEI \times VEI}{m} \times 100 \quad (3)$$

$$\text{mass of pure biodiesel, } Y = \frac{c}{100} \times d \quad (4)$$

where c refers to the ester content or purity of FAME in the biodiesel sample, TA the total area, AEI the area of internal standard, CEI the concentration (mg/mL) of methyl heptadecanoate solution, VEI the volume (mL) of methyl heptadecanoate solution and m the mass of the sample. To obtain the mass of pure biodiesel, Equation 4 was applied using the ester

content value obtained previously in Equation 3. Lastly, the percentage of pure biodiesel was calculated using Equation 5.

$$\% \text{ Pure Biodiesel, } B = \frac{Y(g)}{A(g)} \times 100\% \quad (5)$$

RESULTS AND DISCUSSION

Thermogravimetry (TGA-DTG) Analysis

To study the influence of calcination temperature on weight loss, KOH and K_2CO_3 catalysts supported with Al_2O_3 powder were subjected to thermal analysis from 35°C to 1000°C at a heating rate of 15°C/min in a N_2 atmosphere. As can be seen from Figure 2, the TG profile of K_2CO_3/Al_2O_3 displays three weight loss events. The preliminary weight loss of 0.8% for 30 % K_2CO_3/Al_2O_3 was observed at 32-200 °C. This indicates the weight loss of water molecules from evaporation of adsorbed water [34]. The decomposition of $KAl(CO_3)(OH)_2$ that unlocks the OH structure to form K-Al-OH is shown at 200-700°C [35]. The second weight loss of 0.4% was caused by the dehydroxylation of OH molecules at 700°C to form K-Al-O [36]. At temperatures higher than 700°C, the K-Al-O structure starts to be transformed into K_2O_2 and K_2O . The formation of K_2O_2 and K_2O is supported by the XRD data in Figure 3.

KOH/Al_2O_3 shows three stages of thermal decomposition. The first stage at 32-200°C was assigned to the loss of water molecules and the second between 200-400°C was assigned to the decomposition of $KAl(CO_3)(OH)_2$. Thus, the formation of K_2O_2 and K_2O can be observed starting at 650°C and the best calcination temperature for both KOH/Al_2O_3 and K_2CO_3/Al_2O_3 catalysts was 700°C. Besides, increasing the catalyst concentration resulted in the desorption of weight loss of the catalyst [37]. At 1000°C, the catalyst degradation becomes uniform and shows that the catalyst is stable and suitable to be used for the reaction.

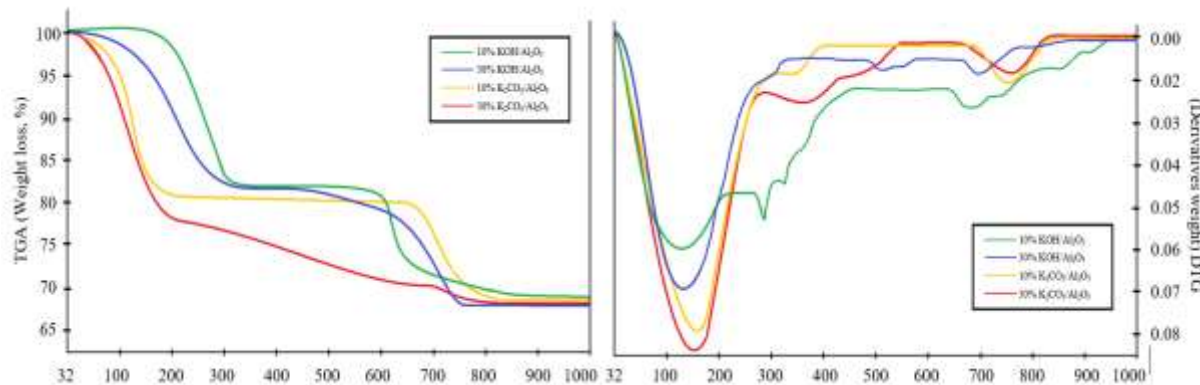


Figure 2. TGA-DTG curves of KOH/Al_2O_3 and K_2CO_3/Al_2O_3 powder catalysts

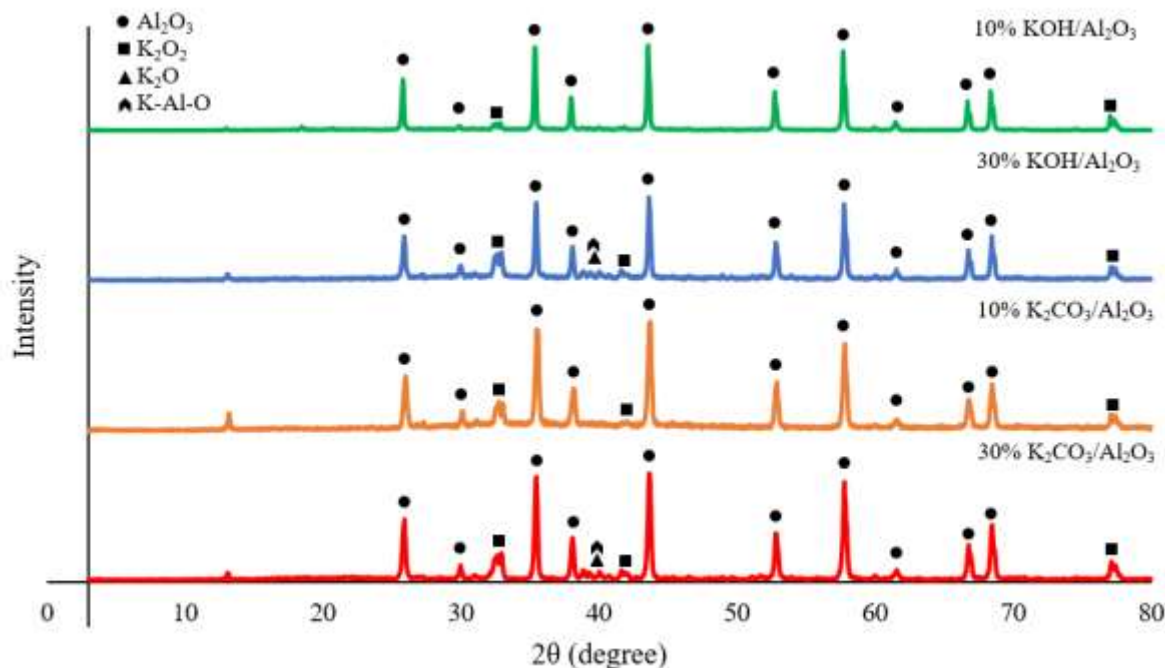


Figure 3 The XRD patterns of KOH/Al_2O_3 and K_2CO_3/Al_2O_3 powder catalysts

X-Ray Diffraction (XRD) Analysis

The XRD patterns of KOH/Al_2O_3 and K_2CO_3/Al_2O_3 powder catalysts are illustrated in Figure 3. The peaks for 10% KOH/Al_2O_3 and K_2CO_3/Al_2O_3 catalysts are less intense compared to the 30% KOH/Al_2O_3 and K_2CO_3/Al_2O_3 catalysts. When the catalyst concentration is increased, the intensities and positions of the peaks change, and the crystal structure of the catalyst becomes sharper. Moreover, the higher intensity will change the crystallinity of the catalyst as new active species K_2O and $K-Al-O$ are observed on the surface of the catalyst [38]. From JCPDS file ((10-0173) and (51-0769)), the peaks at $2\theta = 26^\circ, 30^\circ, 35^\circ, 38^\circ, 44^\circ, 53^\circ, 58^\circ, 67^\circ$ and 69° were assigned to the Al_2O_3 . The formation of K_2O_2 is clearly observed at $2\theta = 33^\circ, 42^\circ$ and 78° (JCPDS file (50-05241)). In addition, when the K_2CO_3 loading was increased to 30%, the new phases of K_2O and $K-Al-O$ were clearly observed at $2\theta = 38^\circ - 40^\circ$ (JCPDS file (53-0809) and (26-1327) respectively).

Catalyst Surface Area and Porosity Characterization

The surface area, size, and porosity characterization of the powdered KOH/Al_2O_3 and K_2CO_3/Al_2O_3 catalysts are summarized in Table 2. The BET surface area, pore size, and pore volume of the 10% catalyst sample were $55.73 \text{ m}^2\text{g}^{-1}$, 8.03 nm, $0.1370 \text{ cm}^3\text{g}^{-1}$ for K_2CO_3/Al_2O_3 and $1.12 \text{ m}^2\text{g}^{-1}$, 12.29 nm, and $0.0853 \text{ cm}^3\text{g}^{-1}$ for KOH/Al_2O_3 respectively. When the concentrations of the powdered KOH/Al_2O_3 and K_2CO_3/Al_2O_3 catalysts were increased to 30%, the surface area, pore size and pore volume were decreased. The BET results were $0.94 \text{ m}^2\text{g}^{-1}$, 15.70 nm, $0.029 \text{ cm}^3\text{g}^{-1}$ for K_2CO_3/Al_2O_3 and $0.12 \text{ m}^2\text{g}^{-1}$, 27.40 nm, and $0.0033 \text{ cm}^3\text{g}^{-1}$ for KOH/Al_2O_3 respectively. A larger surface area will increase the efficiency of the catalyst [36]. Theoretically, IUPAC states that a pore size between 2 to 50 nm indicates a mesoporous structure [10] and from Table 2, all the catalysts are within mesoporous range.

Table 2. Surface area, size and porosity characterization of powder KOH/Al_2O_3 and K_2CO_3/Al_2O_3

Catalyst	Surface area (m^2/g)*	Pore volume (cm^3/g)**	Pore Size (nm)**
10% K_2CO_3/Al_2O_3	55.73	0.1370	8.03 nm
30% K_2CO_3/Al_2O_3	0.94	0.029	15.70 nm
10% KOH/Al_2O_3	1.12	0.0853	12.29 nm
30% KOH/Al_2O_3	0.12	0.0033	27.40 nm

* BET surface area

** Estimated from Barrett, Joyner and Halenda (BJH).

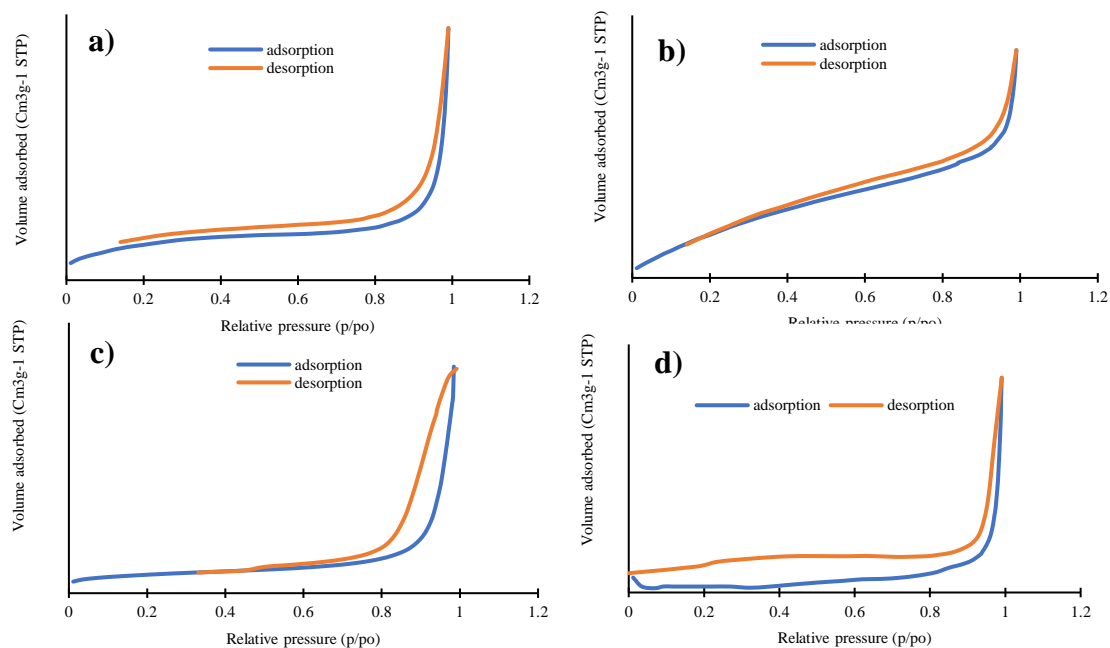


Figure 4. N_2 adsorption-desorption isotherms of calcined a) 10% KOH/Al_2O_3 , b) 10% K_2CO_3/Al_2O_3 , c) 30% KOH/Al_2O_3 , d) 30% K_2CO_3/Al_2O_3

Thus, it is easy for substances such as triglycerides that have a molecular size of 2.5 nm to penetrate the pores on the surface of the catalyst. From the pore volume results for both catalysts, we note that the pore volume decreased with an increase in the catalyst concentration. This is because the support pores are filled with the active phase compound, thus reducing the surface area and pore volume [29]. The change in pore size with catalyst concentration is different compared to the trend for pore volume and surface area. This is because the active phase compound is deposited on the edge of the pores, thus making the pore volume smaller but the pore size larger [21,31]. The adsorption isotherm plots for all catalysts show a Type IV isotherm and a Type B (slit shape) hysteresis loop (Figure 4).

Percentage of ester content and purity of biodiesel sample

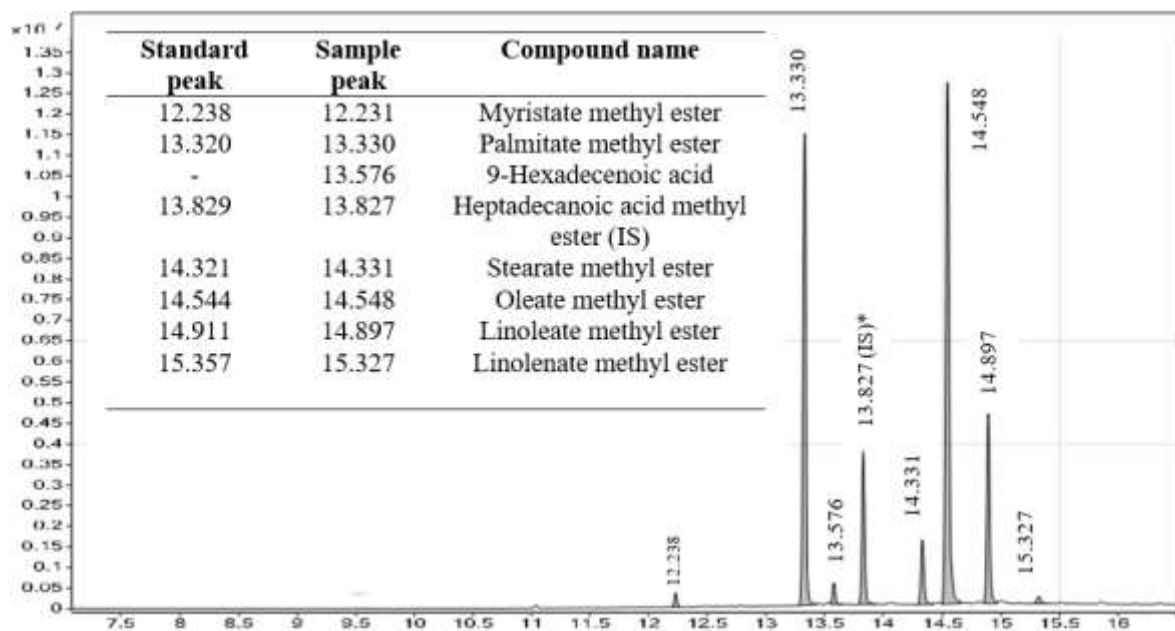
The biodiesel collected after transesterification was further analysed by GC-MS to calculate its actual FAME content. Figure 5 shows the GC-MS peak areas and intensities and the matched compounds.

Methyl heptadecanoate (C17) was used as the internal standard to calculate the ester content in the sample based on the peak areas of the FAME species. The ester content was calculated using equation (2) as mentioned in section 2.6 (EN14103). A sample of 10% K_2CO_3/Al_2O_3 catalyst analysed by GC-MS and the result is shown in Figure 5. Eight peaks were present in the biodiesel, of which only seven corresponded to a methyl ester group. The identified FAME were analyzed against the standard peaks from

a pure biodiesel sample (internal standard) of myristate methyl ester, palmitate methyl ester, stearate methyl ester, oleate methyl ester, linoleate methyl ester, linolenate methyl ester and heptadecanoic acid methyl ester. All peaks that appeared (except for 9-hexadecanoic acid) were verified against different esters and confirmed using the mass spectroscopy (MS) library programme. To obtain more details on the sample, a standard (100% pure biodiesel) was tested and used as a benchmark for the selection of the right peaks to calculate the ester yield in the impure biodiesel.

Biodiesel analysis for transesterification process

The catalysts used for testing WCO in this study were 10 % and 30% K_2CO_3/Al_2O_3 and KOH/Al_2O_3 . The optimum conditions for the transesterification process per 10 grams of WCO were an oil to methanol ratio of 1:12, catalyst loading of 5 wt%, reaction temperature of 65°C and reaction time of 3 hours. Figure 6 shows the results for biodiesel conversion, ester content and biodiesel yield. Biodiesel conversion refers to the biodiesel collected after transesterification process [39]. However, biodiesel conversion cannot represent the true result because the biodiesel collected might consist of impurities such as micro water droplets, glycerol droplets, unreacted TG and methanol droplets [32,40,41]. After the transesterification process, the biodiesel sample must be washed with hot water several times before determining the ester content [18,42,43]. Ester content was determined and calculated by using GCMS while the biodiesel yield was calculated based on its ester content (Equations 4 and 5).



(IS)* : Internal Standard

Figure 5. GC-MS peak areas, intensities and matched compounds for each peak in biodiesel obtained using a 10% K_2CO_3/Al_2O_3 catalyst

The data clearly shows that biodiesel conversion from WCO via transesterification with the aid of 10% K_2CO_3/Al_2O_3 and 10% KOH/Al_2O_3 catalyst were 98.6% and 85%, respectively. When the catalyst concentration was increased (30%), the biodiesel conversion decreased to 80.1% and 70.3%. This is because a larger surface area and pore volume of the catalyst enhanced the reaction of triglyceride at the catalyst's surface. This is also supported by the BET results in Table 2. Between K_2CO_3/Al_2O_3 and KOH/Al_2O_3 catalysts, a highest ester content was obtained using KOH/Al_2O_3 . 30% KOH/Al_2O_3 catalyst gave 94.86% and 30% KOH/Al_2O_3 gave 94.86% ester content. However, the ester content obtained with the 30% KOH/Al_2O_3 catalyst is the

highest because the catalyst is more stable at high concentration, which results in a higher conversion to ester [22]. The 30% K_2CO_3/Al_2O_3 catalyst leached out and dissolved into the biodiesel sample, thus changing the mechanism of the reaction [12,15,31]. The 30% K_2CO_3/Al_2O_3 catalyst easily leached out from the catalyst support, A study by Boonprasop *et al.*, [44] reported that K_2CO_3/Al_2O_3 as a heterogeneous catalyst helped in increasing the biodiesel yield but as the catalyst concentration was increased to 12 wt%, it started to leach out. In summary, the biodiesel yield results showed that 10% catalyst concentration of K_2CO_3/Al_2O_3 and KOH/Al_2O_3 produced the highest yields, which were 87.57% and 77.55%, respectively.

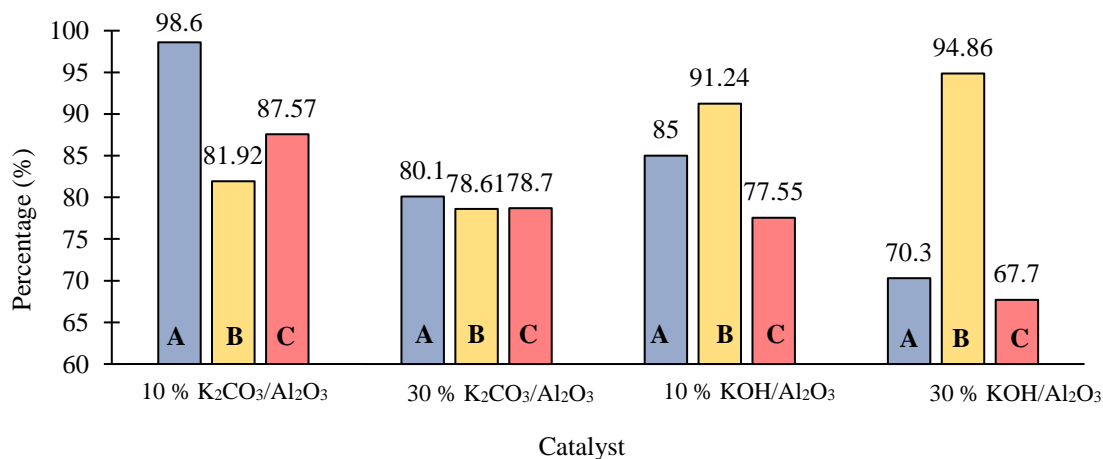


Figure 6. The results obtained using KOH/Al_2O_3 and K_2CO_3/Al_2O_3 powder catalysts for A) Biodiesel conversion, B) Ester content and C) Biodiesel yield

CONCLUSION

The K_2CO_3/Al_2O_3 and KOH/Al_2O_3 powder catalysts successfully converted WCO to biodiesel via a transesterification process under constant reaction conditions (oil to methanol ratio of 1:12, catalyst loading of 5 wt%, reaction temperature of 65 °C with reaction time of 3 hours). The catalyst was prepared by the incipient wetness impregnation method with concentrations of 10% and 30%. The highest yield of pure biodiesel recorded was 87.57% for 10% K_2CO_3/Al_2O_3 and 77.55% for 10% KOH/Al_2O_3 , and both catalysts showed crystalline structures. Based on these results, the catalysts used proved to be effective in recycling WCO to produce biodiesel at minimal cost and in a short period of time. The catalysts were also found to be stable within 3 hours of reaction time and could be easily recovered, thus suitable for industrial applications.

ACKNOWLEDGMENT

The authors acknowledge the funding from Research Grant, FRGS Grant No.: 011000190001 (File no.:600 IRMI/FRGS 5/3(108/2019)).

REFERENCES

1. Dorado, M. P., Ballesteros, E., Arnal, J. M., Gómez, J., López, F. J. (2003) Exhaust emissions from a Diesel engine fueled with transesterified waste olive oil. *Fuel*, **82**, 1311–1315. [https://doi.org/10.1016/S0016-2361\(03\)00034-6](https://doi.org/10.1016/S0016-2361(03)00034-6).
2. Mahesh, S. E., Ramanathan, A., Begum, K. M. M. S., Narayanan, A. (2015) Biodiesel production from waste cooking oil using KBr impregnated CaO as catalyst, *Energy Convers. Manag.*, **91**, 442–450. <https://doi.org/10.1016/j.enconman.2014.12.031>.
3. Mansir, N., Taufiq-Yap, Y. H., Rashid, U., Lokman, I. M. (2017) Investigation of heterogeneous solid acid catalyst performance on low grade feedstocks for biodiesel production: A review, *Energy Convers. Manag.*, **141**, 171–182. <https://doi.org/10.1016/j.enconman.2016.07.037>.
4. Kumar, D., Das, T., Giri, B. S., Rene, E. R., Verma, B. (2019) Biodiesel production from hybrid non-edible oil using bio-support beads immobilized with lipase from *Pseudomonas cepacia*. *Fuel*, **255**, 115801. <https://doi.org/10.1016/j.fuel.115801>.
5. Borah, M. J., Das, A., Das, V., Bhuyan, N., Deka, D. (2019) Transesterification of waste cooking oil for biodiesel production catalyzed by Zn substituted waste egg shell derived CaO nanocatalyst. *Fuel*, **242**, 345–354. <https://doi.org/10.1016/j.fuel.2019.01.060>.
6. Satinah Awang, Z., Ara Arianti, Noor Hidayah, Noor Sairah, Mazni, Rengasamy, T. (2015) Kesedaran Kitar Semula Sisa Minyak Masak dalam Kalangan Pelajar Sarjana Pendidikan Sains Universiti Kebangsaan Malaysia, **18**, 45–52.
7. Ruhul, A. M., Kalam, M. A., Masjuki, H. H., Fattah, I. M. R., Reham, S. S., Rashed, M. M. (2015) State of the art of biodiesel production processes: A review of the heterogeneous catalyst. *RSC Adv.*, **5**, 101023–101044. <https://doi.org/10.1039/c5ra09862a>.
8. Wu, L., Wei, T. Y., Tong, Z. F., Zou, Y., Lin, Z. J., Sun, J. H. (2016) Bentonite-enhanced biodiesel production by NaOH-catalyzed transesterification of soybean oil with methanol, *Fuel Process. Technol.*, **144**, 334–340. <https://doi.org/10.1016/j.fuproc.2015.12.017>.
9. Sharma, Y. C., Singh, B., Korstad, J. (2011) Latest developments on application of heterogenous basic catalysts for an efficient and eco friendly synthesis of biodiesel: A review. *Fuel*, **90**, 1309–1324. <https://doi.org/10.1016/j.fuel.2010.10.015>.
10. Boz, N., Degirmenbasi, N., Kalyon, D. M. (2013) Transesterification of canola oil to biodiesel using calcium bentonite functionalized with K compounds. *Appl. Catal. B. Environ.*, **138–139**, 236–242. <https://doi.org/10.1016/j.apcatb.2013.02.043>.
11. Alonso, D. M., Mariscal, R., Moreno-Tost, R., Poves, M. D. Z., Granados, M. L. (2007) Potassium leaching during triglyceride transesterification using $K/\gamma-Al_2O_3$ catalysts. *Catal. Commun.*, **8**, 2074–2080. <https://doi.org/10.1016/j.catcom.2007.04.003>.
12. Ilgen, O., Akin, A. N. (2009) Development of alumina supported alkaline catalysts used for biodiesel production. *Turkish J. Chem.*, **33**, 281–287. <https://doi.org/10.3906/kim-0809-29>.
13. Islam, A., Taufiq-Yap, Y. H., Ravindra, P., Teo, S. H., Sivasangar, S., Chan, E. S. (2015) Biodiesel synthesis over millimetric $\gamma-Al_2O_3/KI$ catalyst. *Energy*, **89**, 965–973. <https://doi.org/10.1016/j.energy.2015.06.036>.
14. Li, X. F., Zuo, Y., Zhang, Y., Fu, Y., Guo, Q. X. (2013) In situ preparation of K_2CO_3 supported Kraft lignin activated carbon as solid base catalyst for biodiesel production. *Fuel*, **113**, 435–442. <https://doi.org/10.1016/j.fuel.2013.06.008>.
15. Nayebzadeh, H., Haghighi, M., Saghatoleslami, N., Alaei, S., Yousefi, S. (2019) Texture/phase evolution during plasma treatment of microwave-combustion synthesized KOH/Ca

- 12Al14O33-C nanocatalyst for reusability enhancement in conversion of canola oil to biodiesel, *Renew. Energy*, **139**, 28–39. <https://doi.org/10.1016/j.renene.2019.01.122>.
16. Nayeبزadeh, H., Saghatoleslami, N., Tabasizadeh, M. (2016) Optimization of the activity of $KOH/calcium\ aluminate$ nanocatalyst for biodiesel production using response surface methodology. *J. Taiwan Inst. Chem. Eng.*, **68**, 379–386. <https://doi.org/10.1016/j.jtice.2016.09.041>.
17. Nayeبزadeh, H., Saghatoleslami, N., Haghighi, M., Tabasizadeh, M. (2019) Catalytic Activity of $KOH-CaO-Al_2O_3$ Nanocomposites in Biodiesel Production: Impact of Preparation Method. *Int. J. Self-Propagating High-Temperature Synth.*, **28**, 18–27. <https://doi.org/10.3103/S1061386219010102>.
18. Da Costa Evangelista, J. P., Gondim, A. D., Di Souza, L., Araujo, A. S. (2016) Alumina-supported potassium compounds as heterogeneous catalysts for biodiesel production: A review. *Renew. Sustain. Energy Rev.*, **59**, 887–894. <https://doi.org/10.1016/j.rser.2016.01.061>.
19. Puspa Asri, N., Puspita Sari, D. A. (2015) Pre-Treatment of Waste Frying Oils for Biodiesel Production. *Mod. Appl. Sci.*, **9**, 99. <https://doi.org/10.5539/mas.v9n7p99>.
20. Lani, N. S., Ngadi, N., Yahya, N. Y., Rahman, R. A. (2017) Synthesis, characterization and performance of silica impregnated calcium oxide as heterogeneous catalyst in biodiesel production. *J. Clean. Prod.*, **146**, 116–124. <https://doi.org/10.1016/j.jclepro.2016.06.058>.
21. Mutreja, V., Singh, S., Ali, A. (2011) Biodiesel from mutton fat using KOH impregnated MgO as heterogeneous catalysts. *Renew. Energy*, **36**, 2253–2258. <https://doi.org/10.1016/j.renene.2011.01.019>.
22. Rashid, U., Anwar, F. (2008) Production of biodiesel through optimized alkaline-catalyzed transesterification of rapeseed oil. *Fuel*, **87**, 265–273. <https://doi.org/10.1016/j.fuel.2007.05.003>.
23. Silveira, E. G., Barcelos, L. F. T., Perez, V. H., Justo, O. R., Ramirez, L. C., de M. Rêgo Filho, L., de Castro, M. P. P. (2019) Biodiesel production from non-edible forage turnip oil by extruded catalyst. *Ind. Crops Prod.*, **139**, 111503. <https://doi.org/10.1016/j.indcrop.2019.111503>.
24. Hayyan, A., Alam, M. Z., Mirghani, M. E. S., Kabbashi, N. A., Hakimi, N. I. N. M., Siran, Y. M., Tahiruddin S. (2010) Sludge palm oil as a renewable raw material for biodiesel production by two-step processes. *Bioresour. Technol.*, **101**, 7804–7811. <https://doi.org/10.1016/j.biortech.2010.05.045>.
25. Bozorgpour, F., Ramandi, H. F., Jafari, P., Samadi, S., Yazd, S. S., Aliabadi, M. (2016) Removal of nitrate and phosphate using chitosan/ Al_2O_3/Fe_3O_4 composite nanofibrous adsorbent: Comparison with chitosan/ Al_2O_3/Fe_3O_4 beads. *Int. J. Biol. Macromol.*, **93**, 557–565. <https://doi.org/10.1016/j.ijbiomac.2016.09.015>.
26. Ma, H., Li, S., Wang, B., Wang, R., Tian, S. (2008) Transesterification of Rapeseed Oil for Synthesizing Biodiesel by $K/KOH/\gamma-Al_2O_3$ as Heterogeneous Base Catalyst. *JAOCs, J. Am. Oil Chem. Soc.*, **85**, 263–270. <https://doi.org/10.1007/s11746-007-1188-4>.
27. Jamil, F., Murphin Kumar, P. S., Al-Haj, L., Tay Zar Myint, M., Al-Muhtaseb, A. H. (2020) Heterogeneous carbon-based catalyst modified by alkaline earth metal oxides for biodiesel production: Parametric and kinetic study. *Energy Convers. Manag. X*, **100047**. <https://doi.org/10.1016/j.ecmx.2020.100047>.
28. Schlögl, R. (2015) Heterogeneous catalysis. *Angew. Chemie - Int. Ed.*, **54**, 3465–3520. <https://doi.org/10.1002/anie.201410738>.
29. Silveira Junior, E. G., Perez, V. H., Reyero, I., Serrano-Lotina, A., Justo, O. R. (2019) Biodiesel production from heterogeneous catalysts based K_2CO_3 supported on extruded $\Gamma-Al_2O_3$. *Fuel*, **241**, 311–318. <https://doi.org/10.1016/j.fuel.2018.12.074>.
30. Ma, G., Hu, W., Pei, H., Jiang, L., Ji, Y., Mu, R. (2015) Study of KOH/Al_2O_3 as heterogeneous catalyst for biodiesel production via in situ transesterification from microalgae. *Environ. Technol. (United Kingdom)*, **36**, 622–627. <https://doi.org/10.1080/09593330.2014.954629>.
31. Noiroj, K., Intarapong, P., Luengnaruemitchai, A., Jai-In, S. (2009) A comparative study of KOH/Al_2O_3 and KOH/NaY catalysts for biodiesel production via transesterification from palm oil. *Renew. Energy*, **34**, 1145–1150. <https://doi.org/10.1016/j.renene.2008.06.015>.
32. Labib, T. M., Hawash, S. I., El-Khatib, K. M., Sharaky, A. M., El Diwani, G. I., Abdel Kader, E. (2013) Kinetic study and techno-economic indicators for base catalyzed transesterification of *Jatropha* oil. *Egypt. J. Pet.*, **22**, 9–16. <https://doi.org/10.1016/j.ejpe.2012.06.001>.
33. AENOR, Determination of Total FAME and

- Linolenic Acid Methyl Esters in Biodiesel According to EN-14103, [Http://www.aenor.es/6584](http://www.aenor.es/6584) (2011) 16.
34. Nisar, J., Razaq, R., Farooq, M., Iqbal, M., Khan, R. A., Sayed, M., Shah, A., ur Rahman, I. (2017) Enhanced biodiesel production from Jatropha oil using calcined waste animal bones as catalyst. *Renew. Energy*, **101**, 111–119. <https://doi.org/10.1016/j.renene.2016.08.048>.
35. Veselovskaya, J. V., Derevschikov, V. S., Kardash, T. Y., Stonkus, O. A., Trubitsina T. A., Okunev A. G. (2013) Direct CO₂ capture from ambient air using K_2CO_3/Al_2O_3 composite sorbent. *Int. J. Greenh. Gas Control*, **17**, 332–340. <https://doi.org/10.1016/j.ijggc.2013.05.006>.
36. Shan, R., Shi, J., Yan, B., Chen, G., Yao, J., Liu, C. (2016) Transesterification of palm oil to fatty acids methyl ester using K_2CO_3 /palygorskite catalyst. *Energy Convers. Manag.*, **116**, 142–149. <https://doi.org/10.1016/j.enconman.2016.02.084>.
37. Hazmi, B., Rashid, U., Taufiq-Yap, Y. H., Ibrahim, M .L. (2020) Supermagnetic Nano-Bifunctional Catalyst from Rice Husk: Synthesis, Characterization and Application for Conversion of Used Cooking Oil to Biodiesel.
38. Abdelhady, H. H., Elazab, H. A., Ewais, E. M., Saber, M., El-Deab, M. S. (2020) Efficient catalytic production of biodiesel using nano-sized sugar beet agro-industrial waste. *Fuel*, **261**, 116481. <https://doi.org/10.1016/j.fuel.2019.116481>.
39. Koberg, M., Gedanken, A. (2013) Using Microwave Radiation and SrO as a Catalyst for the Complete Conversion of Oils, Cooked Oils, and Microalgae to Biodiesel. *Elsevier B. V.* <https://doi.org/10.1016/B978-0-444-53878-9.00010-2>.
40. Vargas, E. M., Neves, M. C., Tarelho, L. A. C., Nunes, M. I. (2019) Solid catalysts obtained from wastes for FAME production using mixtures of refined palm oil and waste cooking oils. *Renew. Energy*, 873–883. <https://doi.org/10.1016/j.renene.2019.01.048>.
41. Ganesan, S., Arunkumar, T., Munuswamy, D., Appavu, P., Devarajan, Y. (2019) Effect of egr & nanoparticles on performance and emission characteristics of a diesel engine fuelled with palm biodiesel and diesel blends. *J. Oil Palm Res.*, **31**, 130–137. <https://doi.org/10.21894/fjopr.2018.0065>.
42. Suh, W. I., Mishra, S. K., Kim, T. H., Farooq, W., Moon, M., Shrivastav, A., Park, M. S., Yang, J. W. (2015) Direct transesterification of wet microalgal biomass for preparation of biodiesel. *Algal Res.*, **12**, 405–411. <https://doi.org/10.1016/j.algal.2015.10.006>.
43. Thiruselvam K., Ganesh V. (2019) Performance and emission analysis of diesel engine using thermal barrier coating and addition of cerium oxide nanoparticles to palm biodiesel. *J. Oil Palm Res.*, **31**, 138–145. <https://doi.org/10.21894/fjopr.2018.0060>.
44. Boonprasop, S., Chalermssinsuwan, B., Piumsomboon, P. (2018) Effect of operating parameters of potassium carbonate supported on gamma alumina ($K_2CO_3/\gamma-Al_2O_3$) on CO₂ capture capacity using depressurized regeneration. *J. Taiwan Inst. Chem. Eng.*, **88**, 215–225. <https://doi.org/10.1016/j.jtice.2018.04.005>.